



**HAL**  
open science

# **GeoForschungsZentrum Anomaly Magnetic Map (GAMMA): A candidate model for the World Digital Magnetic Anomaly Map**

M. Hamoudi, E. Thébault, V. Lesur, M. Manda

► **To cite this version:**

M. Hamoudi, E. Thébault, V. Lesur, M. Manda. GeoForschungsZentrum Anomaly Magnetic Map (GAMMA): A candidate model for the World Digital Magnetic Anomaly Map. *Geochemistry, Geophysics, Geosystems*, 2007, 8, <10.1029/2007GC001638>. <insu-03603184>

**HAL Id: insu-03603184**

**<https://insu.hal.science/insu-03603184v1>**

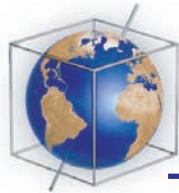
Submitted on 9 Mar 2022

**HAL** is a multi-disciplinary open access archive for the deposit and dissemination of scientific research documents, whether they are published or not. The documents may come from teaching and research institutions in France or abroad, or from public or private research centers.

L'archive ouverte pluridisciplinaire **HAL**, est destinée au dépôt et à la diffusion de documents scientifiques de niveau recherche, publiés ou non, émanant des établissements d'enseignement et de recherche français ou étrangers, des laboratoires publics ou privés.



Copyright - All rights reserved



# GeoForschungsZentrum Anomaly Magnetic Map (GAMMA): A candidate model for the World Digital Magnetic Anomaly Map

**M. Hamoudi**

*GeoForschungsZentrum Potsdam, Telegrafenberg, D-14473 Potsdam, Germany*

*Université des Sciences et de la Technologie Houari Boumediène, BP32 USTHB, 16123, Bab-Ezzouar, Algiers, Algeria*

**E. Thébault**

*GeoForschungsZentrum Potsdam, Telegrafenberg, D-14473 Potsdam, Germany*

*Now at Laboratoire de Géomagnétisme, Institut de Physique du Globe de Paris, 4 Place Jussieu, F-75252 Paris Cedex 05, France (ethebault@ipgp.jussieu.fr)*

**V. Lesur and M. Manda**

*GeoForschungsZentrum Potsdam, Telegrafenberg, D-14473 Potsdam, Germany*

[1] The World Digital Magnetic Anomaly Map (WDMAM) is an ongoing effort toward the mapping of worldwide available aeromagnetic data. It is led by a task force of the International Association for Geomagnetism and Aeronomy (IAGA) and aims at distributing a global map in printed and digital forms. In this paper, we describe in detail our candidate model which has to be evaluated by the IAGA task force together with five other candidate maps. After discussing the quality of the available data, we show a simple but effective method applied to successfully process, reduce, and merge together individual compilations. The near-surface data are corrected using global field models and further refined with two-dimensional polynomial corrections. After the upward continuation to 5 km altitude, data are resampled to a 3 minute grid and merged together. We then calculate a spherical harmonic model up to degree 199 and analyze the magnetic spectrum of the global map. This helps us to confirm that wavelengths larger than 400 km are spurious at a global scale in aeromagnetic compilations. Therefore we substitute them using a satellite-based lithospheric field model (MF5) to degree 100. Finally, our proposed candidate map for WDMAM is presented.

**Components:** 5842 words, 5 figures, 3 tables.

**Keywords:** anomaly map; WDMAM.

**Index Terms:** 1517 Geomagnetism and Paleomagnetism: Magnetic anomalies: modeling and interpretation.

**Received** 20 March 2007; **Accepted** 26 March 2007; **Published** 23 June 2007.

Hamoudi, M., E. Thébault, V. Lesur, and M. Manda (2007), GeoForschungsZentrum Anomaly Magnetic Map (GAMMA): A candidate model for the World Digital Magnetic Anomaly Map, *Geochem. Geophys. Geosyst.*, 8, Q06023, doi:10.1029/2007GC001638.

## 1. Introduction

[2] The importance of aeromagnetic and marine magnetic surveys to understand the geology has been long demonstrated, but a number of problems remain difficult to solve when considering regional compilations only. A worldwide magnetic anomaly model derived from the merging of satellite, airborne, marine and land magnetic data can provide a comprehensive view of continental-scale magnetic trends, not available in individual data sets. It also helps linking widely separated areas of outcrop, unifies disparate tectonic and geological studies [e.g., *Reeves and De Wit*, 2000]. Such a global anomaly map will thus be a powerful tool for further evaluation of the lithospheric structure, geologic processes and tectonic evolution of continental or oceanic areas [*Vine*, 1966]. These studies require consistent data sets over distances of thousands of kilometers spanning national boundaries.

[3] The World Digital Magnetic Anomaly Map (WDMAM) working group of IAGA aims at producing a compiled magnetic anomaly map containing all possible wavelengths useful for geological and tectonic mapping of the crust. The work presented here is a candidate model toward the final WDMAM product. The data sets used in this study were kindly provided by various organizations to the WDMAM committee (see Table 1). These magnetic compilations result from the merging of many independent regional magnetic surveys with various characteristics. Data were recorded at different epochs and altitudes, often without proper secular variation or altitude corrections. The existing final compilations have therefore errors causing significant differences between adjacent panels. These errors are clearly noticeable along the edges of adjacent surveys where leveling errors dominate. As a result, long wavelengths in these surveys are partly spurious and individual compilations do not easily merge.

[4] Large compilations, such as Arctic or the North America grid, extending at scales of several thousands of kilometers are available but, so far, the challenge to handle the number of grids and specifications greatly hampered the attempt to generate a global view of magnetic anomalies. Moreover, most data are still not available for various reasons. Nevertheless, thanks to concerted and persistent efforts during last years, a large number of near-surface magnetic grids are now available and this allows the release of the first magnetic anomaly map.

[5] In a first section, we present the specification of each data sets, the coordinate systems used and, when available, the original main field reduction and the overall statistics. We also report on prominent observed inconsistencies. These discussions help us to define a grid precedence order according to their estimated quality in section 2. In section 3, we present a simple and effective method, applied to merge the individual grids. We correct the large wavelengths by iteratively adjusting a low-degree main field for different epochs until minimum mean anomaly intensity is obtained. We adjust the grid by removing a regional polynomial to the compilation in order to improve the statistical characteristics of each data distribution. Following the recommendation of the WDMAM committee, data are upward continued to 5 km above the World Geodetic System 1984 (WGS84) reference ellipsoid and gridded on a  $3' \times 3'$  grid (about 5 km spacing). We then apply dedicated software in order to knit a compilation at a global scale. After a brief review of different available satellite lithospheric field models, we finally apply a global spherical harmonic filter to the gridded data in order to remove the nonphysical data points, the remaining large wavelength discontinuities and the last inconsistencies. Wavelengths larger than spherical harmonic degree 100, corresponding to 400 km maximum resolution, are removed and the currently best CHAMP anomaly field model available is subsequently added to the grid at 5 km altitude. We finally discuss the GeoForschungsZentrum Anomaly Magnetic Map (GAMMA) map, our candidate model to WDMAM.

## 2. Data Sets

[6] In this project we used the aeromagnetic data provided to us by the WDMAM committee. The available compilations are summarized in Table 1. Some of them are partially redundant and we discuss below how we deal with the overlapping areas.

[7] The overall coverage is especially sparse over oceans, but also over Africa and South America where data exist without being freely accessible. The available data density greatly varies between the Northern and the Southern hemispheres and according to regional characteristics. The data quality over each region is hard to estimate as very few compilations have complete metadata information (see Table 1). When available, metadata information shows compilations to be in different coordinate systems and projections. All compila-

**Table 1.** Data Used in This Study and Available Metadata Information

Compilation Name	Height, m	Coordinate System/Projection	Reduction	References	Index
Antarctic	N/A	Geographic	N/A	ADMAP, <a href="http://www.geology.ohio-state.edu/geophysics/admap/">http://www.geology.ohio-state.edu/geophysics/admap/</a> <i>Verhoef et al.</i> [1996], <a href="http://gsc.nrcan.gc.ca/">http://gsc.nrcan.gc.ca/</a>	47
Arctic compilation	1000	Geographic	Filtered 500 km	<i>Wonik et al.</i> [2001] <i>Le Mouél</i> [1969]	41
Europe	3000	Lambert conic conforme 30/60-20	DGRF1980		17
France	3000	Lambert II étendu	Total field 1964.5		12
China		Geographic	N/A	N/A	
Middle East	1000	Geographic	N/A	AAIME, <a href="http://home.casema.nl/errenwijlens/ite/aaime/">http://home.casema.nl/errenwijlens/ite/aaime/</a> Geoscience Australia, <a href="http://www.ga.gov.au/">http://www.ga.gov.au/</a>	31
Australia	1000	N/A	N/A	N/A	61
USSR	500	Geographic	VSEGEI 1965		
Russia	N/A	N/A	N/A	VSEGEI, <a href="http://www.vsegei.ru/WAY/247038/locale/EN/">http://www.vsegei.ru/WAY/247038/locale/EN/</a>	23
South East Asia		Geographic	N/A	CCOP, <a href="http://www.ccop.or.th">http://www.ccop.or.th</a>	37
North America	varying	NAD27	CM4 varying	NAMAG, <a href="http://pubs.usgs.gov/sm/map_map/">http://pubs.usgs.gov/sm/map_map/</a>	43
South Africa (SaNaBoZi)	1000	Geographic	N/A	SADC, <a href="http://www.sadc.fi">http://www.sadc.fi</a>	71
Italy	0	Geographic	IGRF 1979	<i>Chiappini et al.</i> [2000]	3
Finland	150	WGS84	DGRF-65	GTK, <a href="http://www.gtk.fi">http://www.gtk.fi</a>	7
Fennoscandia		WGS84	DGRF-65	GTK, <a href="http://www.gtk.fi">http://www.gtk.fi</a>	11
Spain	3000	UTM33N	IGRF1987	<i>Socias et al.</i> [1991]	5
Canary Island	3200	UTM 28N	IGRF 1993.79	<i>Socias and Mezcua</i> [1996]	67
Eurasia	5000	Geographic	N/A	GSC, <a href="http://gsc.nrcan.gc.ca">http://gsc.nrcan.gc.ca</a>	29
Austria	5000	GK, M31	N/A	GSA, <a href="http://www.geologie.ac.at">http://www.geologie.ac.at</a>	19
Marine track lines	varying	Geographic	CM4 varying	NGDC, <a href="http://www.ngdc.noaa.gov/mgg/geodas/trackline.html">http://www.ngdc.noaa.gov/mgg/geodas/trackline.html</a>	83
Africa and South America	5000	Geographic	Varying IGRF	GETECH, <a href="http://www.getech.com">http://www.getech.com</a>	89
India	5000	Geographic	N/A	<i>Qureshy</i> [1982]	73
India	5000	Geographic	N/A	GSI, <a href="http://www.gsi.gov.in">http://www.gsi.gov.in</a>	79
Project Magnet	4750	geographic	Comprehensive models	NGDC, <a href="http://www.ngdc.noaa.gov/seg/geomag/proj_mag.shtml">http://www.ngdc.noaa.gov/seg/geomag/proj_mag.shtml</a>	
Argentina inland	5000	N/A	N/A	SEGEMAR, <a href="http://www.segemar.gov.ar">http://www.segemar.gov.ar</a>	53
Argentina margin	5000	Geographic	N/A	Ghidella, DNA, <a href="http://www.dna.gov.ar">http://www.dna.gov.ar</a>	59
MF5	5000	geographic	POMME 3.1	<a href="http://www.gfz-potsdam.de/pb2/pb23/index.html">http://www.gfz-potsdam.de/pb2/pb23/index.html</a>	97

tions result from the stitching together of smaller surveys carried out at various altitudes and the individual panels were, or were not, upward continued to a common altitude. For some compilations, this information is provided but since in general the mean altitude, or the mean terrain clearance with respect to the mean sea level, is not systematically known, we have no other choice but to upward continue the data in the latest stage of the final compilation.

[8] Panels inside each individual compilation were derived for different epochs and reduced with either local polynomials or IGRF/DGRF models. In most cases, it was difficult to find out which model was used to reduce the data. The final patch-worked grids were thus prone to mismatch in anomaly shapes and strengths that may easily be confused with magnetic anomalies. The lack of absolute reference makes it difficult to restore the large wavelengths. Data sampling is also not homogeneous. It varies from about 50 km and 30 km for respectively India and both Africa and South America grids, to 1 km spacing for North America or Australia, for instance. Determining the grid resolution for each compilation would require a full spectral analysis that was not performed here. Checking the consistency between two overlapping grids is therefore challenging in some areas where the actual resolution is not known. Moreover, the resolution is usually not homogeneous within the compilations themselves and some regions artificially appear devoid of small magnetic anomalies. In future WDMAM editions this problem should be identified before any interpretation is carried out.

[9] Three data sets were used for cosmetic reasons until better grids are provided: part of Africa and South America in the Southern hemisphere and the north west of Indian grid constructed from ground stations.

[10] Several versions exist for some compilations. For instance, version 4 of Australian and adjacent marine areas data were considered. In general, redundant panels were simply removed from the final data set if they did not bring resolution improvement. Hence Mexico grid was removed as the data were included in the North American compilation. Japan grid was part of the East Asia compilation and was not considered. To the contrary, Fennoscandia and Austria, included in the Arctic and European compilation, have a better resolution. After a thorough analysis, project Magnet data set was removed over North America and

Australia, in order to minimize the associated spurious effects. Some compilations such as China or Mongolia were obtained from digitization of shaded color maps and thus discarded. In the latter cases, the quality of the grid could not be objectively testified but visual inspections and statistics show discontinuities, noise, unrealistic linear features spreading over thousands of kilometers and obvious edge effects.

[11] Regarding all these aspects, although some grids have interesting characteristics, only a few files like the French, Italian and Spanish grids, for instance, possess the complete information to fully control the data processing. The French grid is also derived from a one-year survey carried out at a nearly constant altitude and reduced to 3 km altitude above mean sea level. Line leveling, main field and external field corrections using the nearest observatory were performed [*Le Mouël*, 1969]. The grid also comes with the total field intensity and, as it slightly overlaps with the European compilation, we used the French data set to level the European compilation near the French boundary. Similarly, the Italian compilation is a corrected grid provided with the regional polynomial used to reduce the total intensity [*Chiappini et al.*, 2000]. It is thus possible to further correct for a global core field model or a given epoch. Information on the core field reduction is not provided for the Australian compilation, it nonetheless provides high quality data consistent over large scale with satellite observations.

[12] Before applying filtering and correction procedures, the data not provided in a geographic coordinate system were converted to the global WGS84 reference ellipsoid using transformation formula [*Snyder*, 1987] and a dedicated software (Oasis Montaj, GeoSoft<sup>©</sup>).

### 3. Grid Inconsistencies and Discontinuities

[13] Some problems discussed above, inherent in each grid, are not directly noticeable but appear simply by displaying the grids on the sphere. Discontinuities are a major issue visible on all compilation edges. It is clearly noticeable at the Northern border between the American compilation and the Arctic compilation, for instance. Regarding the specificities and the varieties of survey composing the American NAMAG compilation, and despite the preliminary CM4 model reduction [*Ravat et al.*, 2003] we expect a poor

**Table 2.** Original Statistics<sup>a</sup>

Grid Name	Grid Size	$\delta F_{\min}$	$\delta F_{\max}$	$\langle \delta F \rangle$	$\sigma$	$\Sigma$
Africa and South America	65030	-1058	633	2.87E + 00	66	86615
Antarctica	969479	-924	2140	8.50E-01	124	823531
Arctic	2225311	-2573	5504	-2.30E-01	167	-514358
Argentina continent	571585	-3225	1416	4.74E-01	108	271092
Argentina margin	44092	-146	313	-7.39E + 00	46	-326009
Australia	793060	-19068	2646	2.69E + 00	138	2129860
Austria	4240	-36	147	1.27E + 01	26	53838
Canary	328077	-309	545	8.66E + 01	95	28420981
East India	625898	-4018	7076	5.20E + 00	102	3272122
Eurasia	1758876	-879	1066	-5.00E-01	120	-803297
Europe	664626	-1689	8035	1.61E + 01	180	10710206
Fennoscandia	78861	-498	1307	1.14E + 01	160	896232
Finland	420121	-2111	4005	1.95E + 00	241	821084
France	7560	-105	254	2.61E + 00	29	19712
Italy	36603	-732	1472	1.17E + 01	79	430837
Magnet Project	7814111	-9571	22527	-1.92E + 01	94	-1498689-01
Marine Data	2379244	-25809	45932	-2.00E + 00	930	-5704980-00
Mexico	79699	-723	718	-1.63E + 02	86	-12962119
Middle East	4915299	-5465	2413	-9.90E-01	97	-4869716
NAMAG	63447385	-22724	27540	5.40E-01	192	34263569
Russia	1061053	-978	9605	5.50E + 01	350	58444363
Sanabozi	12324191	-14583	11433	6.37E + 01	176	43554434
South Asia	3554249	-990	2197	-2.75E + 01	84	-9782598-01
Spain	81501	-86	251	1.35E + 01	21	1100325
USSR	14481793	-32685	32560	3.99E + 01	253	578134196

<sup>a</sup> From left to right: Grid name, number of points, minimum and maximum anomaly intensity, standard deviation, and arithmetic sum.

resolution for wavelengths greater than 200 km. The most evident discontinuities are between continental and oceanic compilations. The marine track lines data suffer from data reduction, line leveling and instrumental biases that require a full reprocessing not performed here. The original Canary grid has unrealistic magnitudes that were adjusted using adjacent compilations.

[14] A quick inspection of basic statistics provides further details about the reliability of each data set. The statistics help us to define a precedence order that is later used for merging grids. For some compilations, as shown in Table 2, the average anomaly intensity greatly deviates from zero. If in a first approximation we assume a dominating crustal field for wavelengths smaller than 3000 km (i.e., spherical harmonic degree 15), the intensity anomaly should average to zero over large distances. In that respect, the Russian and the South Asia compilations show peculiar statistics with large anomaly intensity means. This reveals either a poor core field reduction or spurious long wavelengths. The European compilation has also a

comparatively large mean ( $\sim 16$  nT), which leads to large discontinuities with all surrounding compilations. Nevertheless, the metadata information indicates that the European compilation was purposefully reduced with the DGRF1980 and the core field contributions for spherical harmonic degrees 11–15 explain mostly this relatively high mean.

[15] The standard deviation is usually between 100 nT and 200 nT over continents, but the marine data shows a standard deviation reaching 930 nT. This suggests the persistence of noise, bad tracks or outliers. For this reason, the correlation between marine and satellite data is particularly poor. One of the reasons is that marine data are not corrected for external or daily magnetic variations. In addition, the crossover tracks, recorded at different times over long periods, are naturally contaminated by the magnetic secular changes and external fields and large mismatches are observed.

[16] The calculation of the arithmetic sum is informative and shows how well the residuals distribute around the mean. For a pure anomaly field, we

expect a Gaussian-like distribution with zero mean. A non symmetric anomaly distribution around the mean possibly indicates some positive or negative outliers tailing on the distribution. The marine compilation has the larger arithmetic sum closely followed by the Russian, the Australian, and the South Asia compilations. Note that the comparatively high mean for the European compilation does not imply a particularly high arithmetic mean, showing evidence that the European grid does not contain prominent outliers.

#### 4. Partial Correction and Adjustments

[17] This section introduces the preprocessing designed to improve the compatibility in the overlapping areas. We did not systematically analyze the grid consistencies at regional scales except for few oceanic compilations. Most compilations were obtained by combining, locating and processing individual survey to generate a wider compilation. We assumed rather reliable and uniform grid qualities, unless otherwise stated as for the European grid.

##### 4.1. Visual Inspection

[18] A rough technique to smooth the inconsistencies is to bin data on a coarser grid. Here, we kept the original grid as far as possible in our processing and we tried to identify the evident wrong isolated points or track lines.

[19] For the oceanic compilation, we identified bad tracks spreading over thousands of kilometers in the Pacific Ocean and we recorded a maximum anomaly field up to 45931.7 nT. We manually removed these tracks. We also removed track lines crossing the African continents showing possible instrumental deficiencies and/or location problems in the oceanic data. Offshore Senegal, a few cross-shaped anomalies were removed.

[20] In the Getech South American and the African compilations the original data have been decimated. The resulting grids have a poor quality and a low resolution. The Bangui anomaly, for instance, has a rather unusual shape and it is sometimes difficult to delineate clearly other well-known anomalies.

[21] The Indian grid based on repeat stations was considerably reduced and we kept only data following the magnetic map boundaries of *Qureshy* [1982] on the eastern coast.

[22] The European grid was shifted by few kilometers such that its anomaly field coincides with known total intensity anomalies over Germany.

This grid was used only when no other data sets were available over the area.

[23] At last, most of the grids were prone to edge effects possibly caused by either remaining large wavelengths or a Fourier filtering over large distances that was performed at the latest stage of their compilation process. We were not able to properly identify and correct for these effects, some anomalies having unusual shapes and being shifted. Europe and Russia were bounded with a data set having complete metadata information. We were thus able to better constraint the merging between adjacent grids in these regions.

##### 4.2. Global Field Correction

[24] Compilations were formerly reduced with different IGRF/DGRF core field models sometimes followed by two-dimensional polynomial fitting or a Cartesian Fourier filtering. For a few grids over the European continent, we have the correct regional polynomial parameters (or the DGRF model) and sometimes even the total intensity. It was thus easy to add the exact core field model and to remove the CM4 (Comprehensive model [*Sabaka et al.*, 2004]) for the same epoch. For the other compilations, we tried to restore the closest core field model by iteratively looking for the lowest residuals at different epochs after adding a DGRF model (spherical degree 10) and subtracting the CM4 model to degree 15. The complete period between 1960 and 2002 was spanned. The Russian compilation seems to be outside the CM4 time span and the procedure was not applied. Figure 1 shows a few examples and results at this step. The residuals have no particular shape but a minimum can be found (although sometimes not exactly unique). Since we have no information about the removed model, this ad hoc procedure may be arguable. Nevertheless, this step improves the data statistics presented in Table 3 by lowering the mean intensity anomaly toward zero. When considering the total field intensity data, the minimum is obvious. For example, the curve for France shows that the variation of the residual over the 40 years interval is of the magnitude order of the secular variation. The same result is obtained for Italy or Spain. This procedure is thus a way to better correct for the secular variation between the different compilations. Since original data may contain various artifacts caused by the different model biases, it is also a mean to reduce the data with the same core field model. In general, the

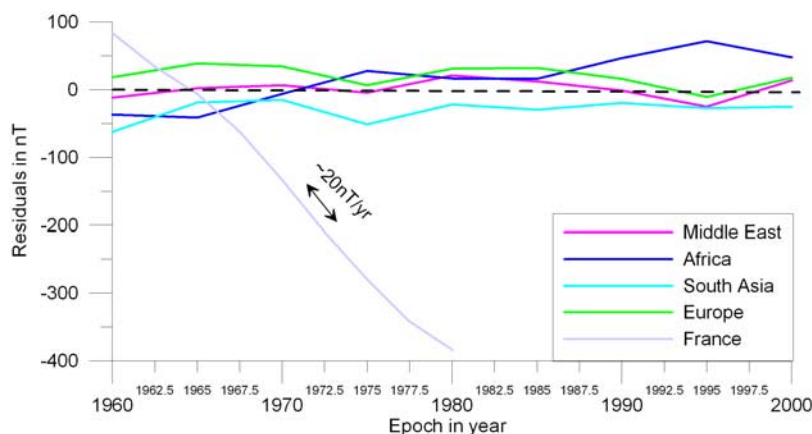


**Figure 1.** Compilations and individual surveys are iteratively corrected from the main field using DGRF and CM4 for each period. The reduction epoch is selected for the minimum anomaly field.

continuity in overlapping areas between adjacent compilations was improved.

### 4.3. Regional Polynomial Correction

[25] In order to further improve the statistics, a regional second order polynomial was removed from all grids in the WGS84 geographic reference so that we avoid Cartesian distortion due to the Earth's curvature. This was not possible over geographic poles and Arctic and Antarctic compilations where the processing procedure was based on using Cartesian reference frame instead. The polynomial fitting was not applied to the Australian compilation where we assumed that the long wavelengths were valid. Removing a polynomial carries the risk of destroying all possible correlation between ground and satellite data as is illustrated below. The spectrum is modified as the polynomial correction is a function of the grid size but wavelengths larger than spherical harmonic degree 100 are ultimately filtered out (see section 4.6). After this correction, the grids have arguably the correct properties characterizing anomaly fields; the average anomaly intensity and the arithmetic sum are almost zero (Table 3) and the residual histograms look like a Gaussian distribution (see Figure 2).

### 4.4. Upward Continuation

[26] The original grids are provided at various but generally constant altitudes within the same data set (see Table 1). This may be not true for some compilations, but this problem could not be addressed here as correct altitudes cannot be recovered. We applied the filter at the specified mean altitude. Oceanic data sets were also upward

continued in order to avoid a too sharp transition between ocean-continent boundaries.

[27] The grids smaller than 2000 km width, like Argentina, Austria, Fennoscandia, Italy, France, Mexico and Spain, were directly upward continued to 5 km altitude above the geoid. Larger compilations were split into 2000 km by 2000 km squares, which were upward continued individually. This dimension corresponds to the maximum size for which the Earth's curvature can be neglected [Nakagawa *et al.*, 1985]. This requires a Nyquist resampling of the original grid on a 2.5 km regular grid in a Cartesian reference frame so that a maximum resolution of 5 km is obtained. The spacing is chosen as to get the best trade-off between speed and efficiency. This high resampling is probably unnecessary as none of the data sets has a true 5 km resolution. The upward continued data are then calculated back to the original geographic data locations. The GeoSoft<sup>©</sup> algorithm includes a detrending of the data and works in the Fourier domain. Each panel slightly overlaps with the adjacent ones and we systematically checked the consistency of the result over the overlapping areas. We cannot report on noticeable distortion, and the overall statistics in Table 3 are nearly preserved. It is worth noting that after the upward continuation the edge effects between adjacent grids were not significantly but slightly enhanced.

### 4.5. Merging the Grids

[28] The merging process does not rely on physical assumptions and whether merging the neighboring grids or not is a matter of choice. We first considered the complete overlap between different grids

**Table 3.** Statistics After Preprocessing and Outlier Correction<sup>a</sup>

Grid Name	Grid Size	$\delta F_{\min}$	$\delta F_{\max}$	$\langle \delta F \rangle$	$\sigma$	$\Sigma$
Africa and South America	65030	-1032	701	1.30E-09	66	3.E-08
Antarctica	969479	-894	2113	6.00E-11	128	6.E-05
Arctic	2225311	-2604	5528	-2.15E-11	171	-5.E-05
Argentina continent	571585	-3150	1480	3.80E-04	107	-1.E-07
Argentina margin	44056	-137	318	1.36E-13	44	6.E-09
Australia	793060	-1482	2237	3.40E-11	150	8.E-04
Austria	4240	-55	137	2.70E-15	27	0.E + 00
Canary	328077	-400	456	3.30E-11	87	1.E-05
East India	625898	-4001	7109	1.30E-11	102	8.E-06
Eurasia	1758876	-916	1034	-2.30E-11	123	4.E-05
Europe	664626	-1712	7983	-1.70E-11	179	1.E-06
Fennoscandia	78862	-526	1254	-7.00E-13	158	6.E-09
Finland	420121	-2110	3974	6.00E-11	240	2.E-05
France	7560	-111	251	3.00E-15	29	0.E + 00
Italy	36603	-747	1402	6.00E-14	79	2.E-09
Magnet Project	7814111	-2000	2000	-3.00E-07	89	0.E + 00
Marine Data	19455835	-2000	2000	-6.00E-12	148	1.E-04
Mexico	79699	-562	876	1.72E-12	86	-1.E-07
Middle East	4915299	-5446	2408	1.10E-11	101	5.E-04
NAMAG	63447385	-22567	26232	4.00E-10	191	3.E-02
Russia	1061053	-1046	9545	-4.29E-11	349	5.E-05
Sanabozi	12324191	-14642	11341	-8.00E-12	176	-1.E-04
South Asia	3554249	-340	2196	1.60E-11	85	6.E-05
Spain	81501	-97	242	7.00E-14	20	0.E + 00
USSR	14481793	-32138	31455	5.00E-10	249	8.E-03

<sup>a</sup>From left to right: Grid name, number of points, minimum and maximum anomaly intensity, standard deviation, and arithmetic sum.

in order to obtain a final grid averaging the full available information. It occurred to us that this procedure was generating spurious long and intermediate wavelengths in the merged data set. Moreover, it gave the same weight to data set of different qualities, which was unacceptable. As a result, not more than 50 km overlap was allowed between redundant data sets. We thus obtained a merged grid smoother and closer to the independent original grids. Large amount of both North America and Arctic compilation data were removed. In South Africa, data were cut when overlapping

SaNaBoZi data set, whereas in South America, they were cut when overlapping Argentina data set.

[29] The preliminary processing from paragraph 4.a to 4.d reduces the large discontinuities but does not fully remove them. We used the grid-knitting tool of GeoSoft<sup>©</sup> in order to smooth out the transition between adjacent grids. Some spurious wavelengths are created that will be mostly filtered out at the last stage of the processing. We were especially careful when choosing the precedence grid order. We already argued that French, Italian, and European grids were easier to process as we

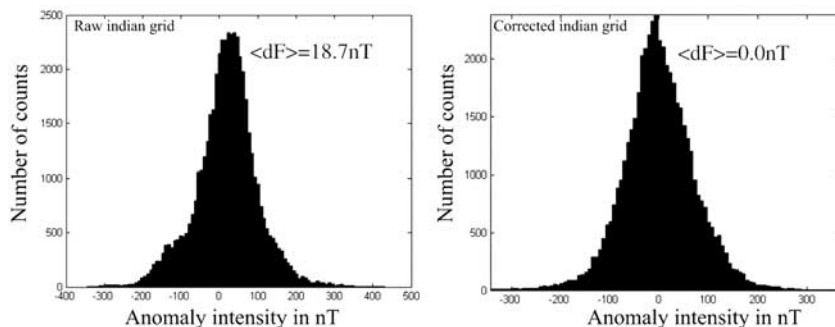


**Figure 2.** Example of an anomaly intensity distribution before and after main field and polynomial corrections for the East Indian grid.

have the necessary metadata information to better control the processing. Merging large compilations with small compilations includes a risk, because the adjustment is better constrained by the large compilation even if the small one has apparently a better quality. Before merging the grids, we generated compilations with comparable grid sizes.

[30] The precedence order was as follows: French, Italian and Spanish grids were first merged together. We then built a second grid from the Finland, Fennoscandian, European and Austrian grids. These two new compilations were merged together and the grid from Russia, Eurasia, Middle East, Antarctica and North America were successively added to the compilation. The remaining grids were not merged as they did not overlap with the grids listed above.

[31] At this stage, a  $3' \times 3'$  grid was generated using GMT [Wessel and Smith, 1991] (version 4.1.4). Each node of our final grid was associated to an index corresponding to the data set used to calculate the anomaly field value at that node (last column of Table 1). When a grid node was associated with several data sets, the given index corresponds to the weighted average of the data sets indices. Compilations without index in Table 1 were not used in our merging. Marine data were interpolated whenever the data density was estimated high enough, otherwise left as single track data.

#### 4.6. Final Global Filtering

[32] Any discontinuity caused by large wavelengths introduced during the merging can be filtered out at a global scale by a spherical harmonic transformation. Compilation boundaries are still visible, especially between Arctic, Oceanic and Australian grids. In addition, the mismatch between European and Russian compilation remains. We thus performed a spherical harmonic transform and filter out wavelengths larger than spherical harmonic degree 100 in our global grid to replace them with a continuous satellite-based model.

[33] Two different techniques were envisaged for filtering and smoothing the final grid. A first option consists in filtering the grid using Fourier transforms. This procedure was relatively fast but is a nonpotential method. Thus the coefficients could not be used for predicting the three components of the magnetic field. Moreover, it was difficult to remove remaining nonphysical magnetic measure-

ments. Here, we considered the magnetic anomaly field as the projection of the crustal field onto a core field model: The grid was interpolated on the knots of the sampling, theorem given by *Driscoll and Healy* [1994]. The parameters up to spherical harmonic degree 199 were obtained by least squares (maximum resolution of 200 km). For higher degrees, the coefficients are difficult to obtain and the processing is time-consuming, as the power is very low. This is due to data gaps and heterogeneous resolution at the global scale. The anomaly field was linearized and projected on the 1990 core field, whose coefficients were extracted from the CM4 model to degree 15 [Sabaka et al., 2004]. It is thus believed that the estimated Gauss coefficients represent better the three components of the magnetic field anomaly. Interestingly, despite our careful preprocessing, the first iteration showed evidence of remaining outliers and non-physical data points, characterized by the presence of strong spikes creating oscillations spreading over large distances. This carries the risk of introducing artificial anomalies at all wavelengths in our final map. Some extra points were thus removed from Argentina, Argentina coastline, near Santa Helena Island and around Madagascar. The procedure was then redone without apparent other artifacts.

[34] In Figure 3 we compare the spectrum of our spherical harmonic model with the most recent lithospheric field models, MF4, MF4x [Lesur and Maus, 2006] and MF5 [Maus et al., 2007]. The near-surface WDMAM spectrum can be divided into three parts. The first part of the spectrum, from degrees 1 to 40, is comparatively steeper, has an excess of power and is more irregular. This suggests that large wavelengths are indeed partly spurious even if the correlation analysis (Figure 4) shows a better agreement than expected (0.5 in average for these degrees). Degrees 41 to 89 are more stable and their variation is consistent with satellite-based spectrum. From degree 90, a small offset is noticeable whose origin remains unclear. We may venture that some recent grids were compiled using a satellite-based model derived to degree 90 as prior information. This could have induced this lack of power. Indeed, MF5 has a lack of power explained by the processing applied to satellite data in order to obtain a robust model from noisy measurements. The spherical harmonic correlation analysis [Langel and Hintze, 1998] between MF5 and our near-surface model (Figure 4) shows an average correlation of 0.61 for all degrees, but again, beyond degree 40 it is more

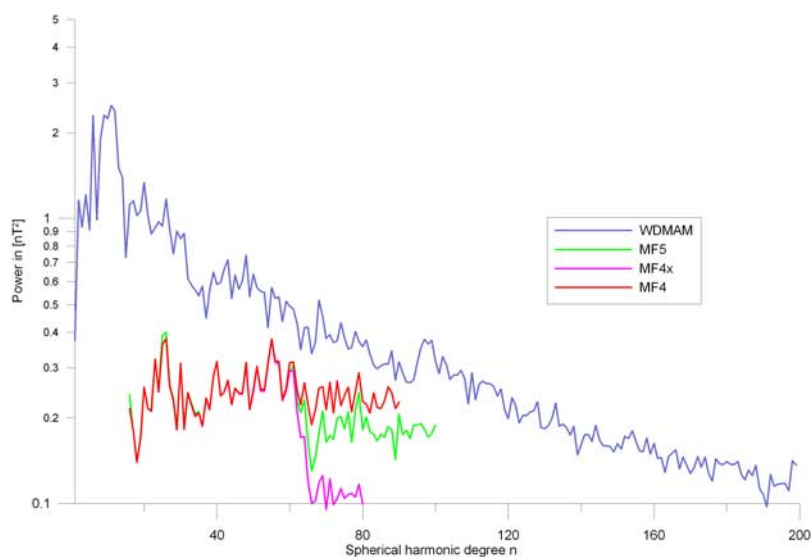


**Figure 3.** Spectra of the near-surface data and satellite-based models. A small increase around degree 90 suggests that some data were reduced with a global field model.

stable and reaches 0.75 (for  $n = 91$ ). We notice a comparatively lack of correlation between degrees 70 and 75 that we do not explain.

## 5. Substitution of Long Wavelengths and Generation of the 3' Grid

[35] In many regions, low-orbiting satellites can map the strength and the extension of the lithospheric field. Choosing a global magnetic lithospheric field model is not a trivial task and a systematic quality analysis is required. For this reason, we discarded the lithospheric field models

based only on satellite missions prior to the Danish Ørsted mission (launched in 1999). *Langel and Hintze* [1998] give a comprehensive overview of earlier satellite missions, such as MAGSAT or POGO and their outcomes, which are not discussed here. The Ørsted satellite was followed by CHAMP (July 2000) and SAC-C (November 2000). Several models, based on these missions sharing comparable scientific instruments, were proposed in the last decade. More details on these three satellite missions, as well as different geomagnetic field models, are given by *Mandea and Purucker* [2005].

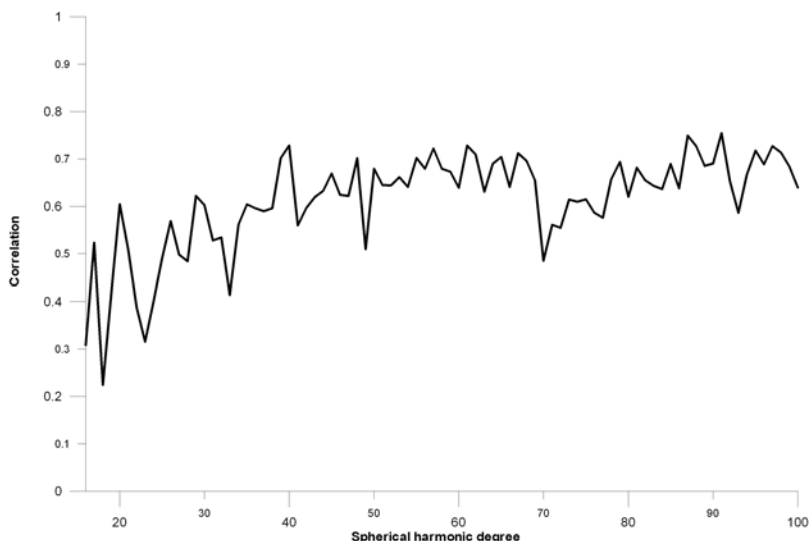


**Figure 4.** Spherical Harmonic Correlation Analysis between ground-based and satellite models shows a stable correlation from degree 40.

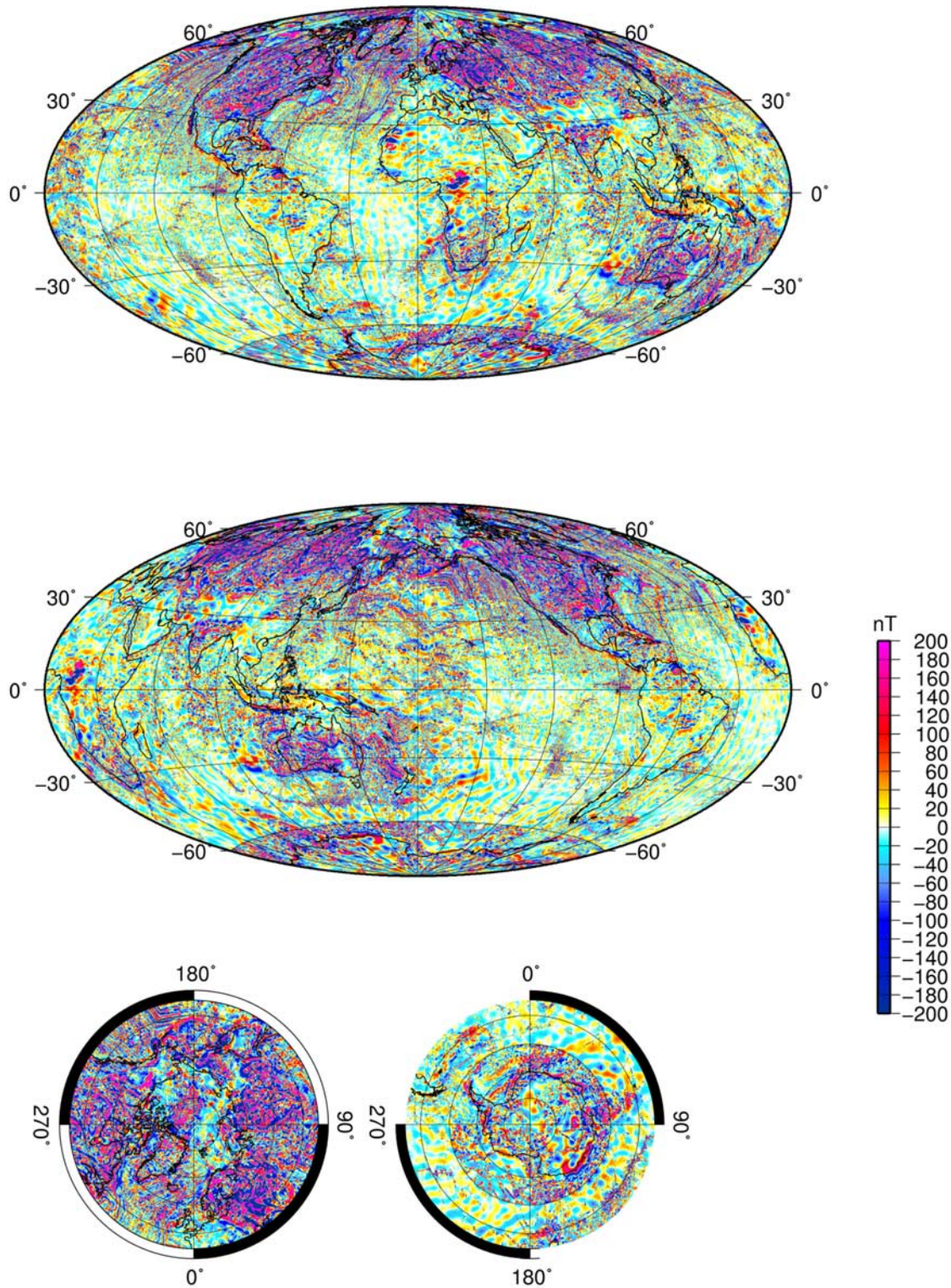


**Figure 5.** Our candidate WDMAM model in a Mollweide projection.

[36] The comprehensive approach (CM4), initiated by *Sabaka et al.* [2004], uses all available data from POGO, MAGSAT, Ørsted, and only scalar data from CHAMP, as well as observatory data, in

order to obtain a global geomagnetic model. Although the model estimates all known sources from the core to the magnetosphere, near-equatorial lithospheric field representation is probably con-

taminated by equatorial electrojet signature due to inclusion of dayside data. Following the same spirit, various magnetic field sources are considered by POMME 3.1 [Maus *et al.*, 2006] using quiet time and night-side data only, which help reducing ionospheric effects and better stabilize the model at the ground level to degree 60. Other models present a very good agreement with this lithospheric field (e.g., CHAOS [Olsen *et al.*, 2006] or BGS/G/L/0706 [Thomson and Lesur, 2007]). These comprehensive approaches give rather robust models for the first degrees but are noisy above degree 50.

[37] Another approach, based on preliminary filtering, strictly focuses on the lithospheric field representation. The philosophy is to carefully select and clean the data for nonlithospheric sources. Maus *et al.* [2006] used this subjective approach with four years of CHAMP data to produce MF4, which is derived up to degree 90. MF4 still shows inconsistencies in the Polar Regions, and Lesur and Maus [2006] managed to constrain independently Polar and Midlatitude regions. Recently, a model up to degree 100 (400 km resolution), using only low orbital CHAMP measurements until mid-2006, was released [Maus *et al.*, 2007]. It is worth noting that data filtering induces a loss of power noticeable when compared with other satellite-based magnetic models but also with aeromagnetic data. Nevertheless, the MF models have degrees that are arguably suitable for large wavelengths replacement and we used MF5 to degree 100 (400 km resolution). These are good compromise between resolution at the ground and smoothness of the lithospheric field at 5 km altitude on the WGS84 ellipsoid. MF5 was thus added to the final grid and our resulting candidate version for the World Digital Magnetic Anomaly Map can be seen in Figure 5. Grid nodes with no aeromagnetic or marine data were filled with MF5 and their index set to 97. The candidate grid with its accompanying notice is available at <http://www.earthref.org/>.

## 6. Conclusion

[38] The World Digital Magnetic Anomaly Map is a promising international effort and an ongoing project. Despite the large disparities between aeromagnetic compilations, we are able to produce a candidate model giving the essence of the worldwide magnetic anomaly distribution. The most important breakthrough to this project will come

with the release of data in uncovered areas. At the present stage, near-surface data gaps are filled in with satellite-based model that may lead to misinterpretation in the shape and strength of the magnetic field. In the future, this problem should be addressed at all scales since data resolution is very heterogeneous even among aeromagnetic grids. Therefore systematic interpretations should be carried out with caution and only a spectral analysis could help identifying the areas of various intrinsic resolutions. A spectral gap is thus presently unavoidable for the wavelengths from 200 km to 400 km.

[39] A major problem was to deal with oceanic data that suffer from large and numerous inconsistencies. In particular, we had to discard project Magnet data that represented too many mismatches with existing data sets. A full crossover analysis of oceanic data will be required in the future that will lead to a better line leveling and resolve the core and external field problems.

[40] Effort continues nowadays to improve both ends of the spectrum and the upcoming Swarm mission configuration will help better resolving smaller wavelengths than degree 100. Other intrinsic problems may arise from compilations and the signal analysis processes; both could introduce artifacts and nonpotential features. In addition to compilation efforts, more elaborated inverse problem techniques are being developed to merge together satellite and ground surface data at regional scales. These techniques, based on Laplace equation, may prove useful to fill the spectral gap, to merge adjacent compilations and to clean the compilation from their nonpotential contributions. The latter are probably of importance as the different grid underwent resampling, decimation and successive nonpotential transformations. In addition, applying a modeling scheme will be useful to homogenize the map resolution.

[41] The first WDMAM edition, considering all candidate models, will be available at <http://www.cgm.org> but future WDMAM editions will greatly benefit from a better spatial coverage, new satellite data and improvements in data processing and modeling.

## Acknowledgments

[42] We are grateful to all organizations that kindly distributed aeromagnetic data to the WDMAM committee. K. Hemant, Monika Korte, and Yoann Quesnel are warmly

acknowledged for their efforts in acquiring various data sets and for useful discussions. This work was supported by the Deutsche Forschungsgemeinschaft (DFG, SPP1097).

## References

- Chiappini, M., A. Meloni, E. Boschi, O. Faggioni, N. Beverini, C. Carmisciano, and I. Marson (2000), On shore-off shore integrated shaded relief magnetic anomaly map at sea level of Italy and surrounding areas, *Ann. Geofis.*, *43*, 983–989.
- Driscoll, J. R., and D. M. Healy (1994), Computing Fourier transforms and convolutions on the 2-sphere, *Adv. Appl. Math.*, *15*, 202–250.
- Langel, R. A., and W. J. Hintze (1998), *The Magnetic Field of the Earth's Lithosphere: The Satellite Perspective*, Cambridge Univ. Press, New York.
- Le Mouél, J. L. (1969), Sur la distribution des éléments magnétiques en France, Ph.D. thesis, Univ. de Paris, Paris.
- Lesur, V., and S. Maus (2006), A global lithospheric magnetic field model with reduced noise level in the Polar Regions, *Geophys. Res. Lett.*, *33*, L13304, doi:10.1029/2006GL025826.
- Mandea, M., and M. Purucker (2005), Measurements of the Earth's magnetic field from space, *Surv. Geophys.*, *26*, 415–459.
- Maus, S., M. Rother, C. Stolle, W. Mai, S. Choi, H. Lühr, D. Cooke, and C. Roth (2006), Third generation of the Potsdam Magnetic Model of the Earth (POMME), *Geochem. Geophys. Geosyst.*, *7*, Q07008, doi:10.1029/2006GC001269.
- Maus, S., H. Lühr, M. Rother, K. Hemant, G. Balasis, P. Ritter, and C. Stolle (2007), Fifth generation lithospheric magnetic field model from CHAMP satellite measurements, Geoforschungszentrum Potsdam, Potsdam, Germany. (Available at <http://www.gfz-potsdam.de/pb2/pb23/index.html>.)
- Nakagawa, I., T. Yukutake, and N. Fukushima (1985), Extraction of magnetic anomalies of crustal origin from Magsat data over the area of Japanese Islands, *J. Geophys. Res.*, *90*, 2609–2615.
- Olsen, N., H. Lühr, T. J. Sabaka, M. Mandea, M. Rother, L. Tøffner-Clausen, and S. Choi (2006), CHAOS—A model of Earth's magnetic field derived from CHAMP, Ørsted, and SAC-C magnetic satellite data, *Geophys. J. Int.*, *166*, 67–75, doi:10.1111/j.1365-246X.2006.02959.x.
- Qureshy, M. N. (1982), Geophysical and Landsat lineament mapping—An approach illustrated from west central and south India, *Photogrammetria*, *37*, 161–184.
- Ravat, D., T. Hildenbrand, and W. Roest (2003), New way of forecasting near-surface magnetic data: The utility of the comprehensive model of the magnetic field, *Leading Edge*, *22*, 784–785.
- Reeves, C. V., and M. De Wit (2000), Making ends meet in Gondwana: Retracing the transforms of the Indian Ocean and reconnecting continental shear zones, *Terra Nova*, *12*, 272–280, doi:10.1046/j.1365-3121.2000.00309.x.
- Sabaka, T. J., N. Olsen, and M. Purucker (2004), Extending comprehensive models of the Earth's magnetic field with Ørsted and CHAMP data, *Geophys. J. Int.*, *159*, 521–547.
- Snyder, J. P. (1987), Map projections—A working manual, *U.S. Geol. Surv. Prof. Pap.*, 1395.
- Socias, I., and J. Mezcua (1996), Levantamiento aeromagnético del archipiélago canario, *Publ. Tec.* *35*, 28 pp., Inst. Geogr. Nacl., Madrid.
- Socias, I., J. Mezcua, J. Lynam, and R. Del Potro (1991), Interpretation of an aeromagnetic survey of the Spanish mainland, *Earth Planet. Sci. Lett.*, *105*(1–3), 55–64.
- Thomson, A., and V. Lesur (2007), An improved geomagnetic data selection algorithm for global geomagnetic field modeling, *Geophys. J. Int.*, doi:10.1111/j.1365-246X.2007.03354.x, in press.
- Verhoef, J. R., R. Macnab, W. Roest, and J. Arkani-Hamed (1996), Magnetic anomalies of the Arctic and North Atlantic oceans and adjacent land areas, *Open File 3125a*, Geol. Surv. of Can., Ontario, Canada.
- Vine, F. J. (1966), Spreading of the ocean floor: New evidence, *Science*, *154*, 1405–1515.
- Wessel, P., and W. H. F. Smith (1991), Free software helps map and display data, *Eos Trans. AGU*, *72*, 441.
- Wonik, T., K. Trippler, H. Geipel, S. Greinwald, and I. Pashkevitch (2001), Magnetic anomaly map for northern, western, and Eastern Europe, *Terra Nova*, *13*(3), 203–213, doi:10.1046/j.1365-3121.2001.00341.x.